Assessing possible dynamical effects of condensate in high resolution climate simulations

J. T. Bacmeister,[1] P. H. Lauritzen,[1] A. Dai,[1] and J. E. Truesdale[1]

Received 2 December 2011; revised 18 January 2012; accepted 18 January 2012; published 23 February 2012.

[1] In areas of heavy precipitation, condensed water species can add significant mass to an atmospheric column. This mass can create positive pressure anomalies of up to several hPa at the surface. This pressure is expected to force a divergent component in the low-level flow that may have an impact on the evolution of the precipitating system. In this study we examine results from a cloud resolving model simulation of tropical convection to estimate the pressure induced by condensates. A simple parameterization of this condensate loading as a function of surface rain rate is derived and implemented in the National Center for Atmospheric Research's Community Atmosphere Model version 5 (CAM5). Our results suggest that at horizontal resolutions of 25 km condensate loading is an important factor in controlling the frequency of intense rain rates in the model. **Citation:** Bacmeister, J. T., P. H. Lauritzen, A. Dai, and J. E. Truesdale (2012), Assessing possible dynamical effects of condensate in high resolution climate simulations, *Geophys. Res. Lett.*, *39*, L04806, doi:10.1029/2011GL050533.

1. Introduction

[2] The contribution of condensed water species to atmospheric mass has long been known to be a significant factor in the dynamics of moist convection [e.g., *Emanuel*, 1994; *Xu and Randall*, 2001]. The weight of condensates in convecting parcels can have a major impact on their buoyancy and may be a dominant control on the global statistics of convection [*Emanuel*, 1994].

[3] The major contribution to condensate mass comes from precipitating species such as rain, hail, snow, and graupel. Microphysics schemes for models at climate resolutions typically use diagnostic rather than prognostic treatments for precipitating condensate. Climate models correctly account for the removal of mass by precipitation in the models' mass budget. However, the diagnostic treatments in climate models view this removal as occurring instantaneously. In reality precipitating condensate may exist in a deep column that persists for a significant time, i.e., comparable to a typical climate model time step of 15 to 30 minutes. The weight of this column contributes to the pressure field (condensate loading, henceforth abbreviated CL) and can have direct dynamical effects on the flow. The dynamical effects of CL are not currently present in most climate models that use diagnostic treatments of precipitation.

[4] Neglect of CL may be justified at the horizontal resolutions of 100's of km. However, as climate model resolution increases we believe this neglect is no longer justified. This study will assess the potential impact of CL at 25 km resolutions by quantifying the condensate contribution to the pressure field in much finer cloud resolving simulations using the National Center for Atmospheric Research's (NCAR's) Weather Research and Forecasting model (WRF) [*Skamarock and Klemp*, 2008]. A simple parameterization of this pressure is developed and implemented in NCAR's Community Atmosphere Model version 5 (CAM5) [*Neale et al.*, 2010]. Our results suggest that horizontal resolutions of 25 km and finer require some representation of CL. This resolution range is already accessible to global climate simulations, and will likely become the default for leading edge simulations in the next ten years. In passing it will be shown that at 25 km and even at 5 km resolutions, CL effects are significantly more important than nonhydrostatic effects.

[5] The paper is structured as follows: In Section 2, we describe the models used in this study. In Section 3 we analyze cloud-resolving model (CRM) results and describe a simple parameterization of CL effects based on surface precipitation rates. In Section 4 we show results from CAM5 including this parameterized CL. In Section 5 we summarize and discuss our results.

2. Models and Experimental Setup

2.1. CAM5

[6] The Community Atmosphere Model version 5 is a state of the art global climate model. Major differences from earlier versions of CAM include a new 2-moment, 2-phase prognostic cloud condensate scheme, advanced boundary layer and shallow convection schemes and deep convection with enhanced plume entrainment and momentum transport. Complete documentation of CAM5 is provided by *Neale et al.* [2010]. In this study we use the finite-volume (FV) dynamical core with a horizontal resolution of 0.23°lat × 0.31°lon and 30 layers in the vertical. A physics time-step of 15 minutes is used. We will examine results from experiments forced by observed sea-surface temperatures (SST) initialized on Jan 1 2005. The experiments ran for 18 months, but in this study we will examine results from the first 13 months only. Currently CAM5 does not incorporate any condensed water species in its atmospheric mass field.

2.2. WRF

[7] The Weather Research and Forecasting model is a well established nonhydrostatic dynamical model with flexible nesting capability [*Skamarock and Klemp*, 2008]. WRF solves the full Euler equations on a dry mass vertical coordinate. Prognostic equations for geopotential, 3D momentum, heat, and water species are included. Pressure is diagnosed from the equation of state [*Skamarock and Klemp*,

[1]NCAR Earth System Laboratory, National Center for Atmospheric Research, Boulder, Colorado, USA.

0094-8276/12/2011GL050533

2008, equation (10)]. In this study we will examine results from the innermost domain of a triply-nested simulation initialized by ERA interim reanalysis.

[8] The simulation period covers February 22 through 27 2005. The innermost domain has a resolution of 500 m in both zonal and meridional directions with a size of 1000 × 800 gridpoints. It is chosen to overlap with the TOGA-COARE domain; 112°E to 117°E and 5°S to 1°S. Fifty vertical levels are used with a top close to 25 km, and Δz ranging from 50 m close the surface to 500 m in the midtroposphere. A 2 second time step is used and data are saved every 15 minutes.

[9] WRF offers a large number of options for parameterizing physical processes, including cloud microphysics. The experiment examined here used the *Hong and Lim* [2006] microphysics option. This is a 6-category bulk scheme that incorporates graupel rather than hail, as appropriate for tropical, oceanic convection. The innermost domain in the simulation discussed here did not employ a deep convection parameterization.

3. Development of Condensate Loading (CL) Parameterization

3.1. Preliminary Analysis of WRF Results

[10] WRF provides a complete pressure field, which includes nonhydrostatic effects and accounts for the complete atmospheric mass field, including the contribution of all condensed water species. Our assessment of the potential CL effect at high climate resolutions (25 km) involves two steps. First, the CRM fields are coarse grained to 25 km resolution by averaging over 50 × 50 gridpoint subdomains. Second, coarse-grained profiles of potential temperature $\bar{\theta}$(K), water vapor mixing ratio with respect to dry air $\bar{q}_w$ (kg kg^{-1}), and condensed water mass mixing ratios with respect to dry air $\bar{q}_{[l,i,r,s,g]}$ (kg kg^{-1}) are calculated. The subscripts l, i, r, s, and g refer to cloud liquid, cloud ice, rain, snow, and graupel. These profiles are used to calculate diagnostic hydrostatic pressure fields with and without CL

$$\bar{\pi}_{hyd,[v,c]}(x,y,z,t) = \bar{\pi}_{top} + \int_z^{z_{top}} \frac{g}{c_p \bar{\theta}_{[v,c]}(x,y,z',t)} dz', \quad (1)$$

where g is the gravitational constant (9.81 m s^{-2}), and c_p is the specific heat capacity of dry air (1004.5 J kg^{-1} K^{-1}). The subscript "v" refers to quantities including virtual effects but not condensate effects, while "c" indicates quantities including both. The model top height z_{top} varies with location and time, but is typically around 25 km. The Exner pressure at the upper boundary $\bar{\pi}_{top} = 0.286$ corresponds to the prescribed model-top pressure of 10 hPa. The Exner pressure π_{hyd} and the pressure are related by

$$\bar{p}_{hyd} = p_{00}\left(\bar{\pi}_{hyd}\right)^{c_p/R}, \quad (2)$$

where R has a value of 287 J kg^{-1} K^{-1}, and p_{00} is a reference pressure of 1000 hPa. We use two versions of thermodynamic variable $\bar{\theta}_{[v,c]}$ in the hydrostatic integral (1)

$$\bar{\theta}_v = \bar{\theta}\frac{1+\bar{q}_w/\epsilon}{1+\bar{q}_w} \quad (3)$$

$$\bar{\theta}_c = \bar{\theta}\frac{1+\bar{q}_w/\epsilon}{1+\bar{q}_w+\bar{q}_l+\bar{q}_i+\bar{q}_r+\bar{q}_s+\bar{q}_g} \quad (4)$$

[e.g., *Emanuel*, 1994, equation (4.3.6)] where $\epsilon = M_{H_2O}/M_{air}$, the ratio of the molecular weights of air and water. With $\bar{\theta}_v$ the diagnostic hydrostatic pressure $\bar{p}_{hyd,v}$ obtained from (1) will include virtual effects but not CL. This quantity is the pressure variable used in most state-of-the-art climate models. Using $\bar{\theta}_c$ in (1) yields an approximate hydrostatic pressure including both virtual effects and CL.

[11] Figure 1 shows joint frequency distributions (JFDs) of $\bar{p}_{hyd,c}$ and $\bar{p}_{hyd,v}$ at the surface versus the coarse grained pressure from WRF $\bar{p}$. Figure 1b shows that ignoring CL even at 25 km resolutions leads to frequent, large surface pressure departures from the WRF value. Underestimates of several hPa are common. A clear implication of this result is that high-resolution climate model surface pressures in regions of strong precipitation may be systematically underestimated by several hPa. In the tropics, pressure anomalies of this size may be dynamically-significant. The CL effect on pressure should act against low-level convergence, and should therefore weaken CISK (Conditional Instability of the Second Kind)-interactions between moist heating and flow in the boundary layer.

[12] The close agreement between $\bar{p}_{hyd,c}$ and $\bar{p}$ in Figure 1a implies that nonhydrostatic dynamics are unimportant at the 25 km scale. So, while small, intense, nonhydrostatic updrafts may be critical in determining vertical fluxes, their detailed structure has negligible impact on the pressure field at scales of 25 km. Based on this analysis there is no reason to suspect that explicitly-resolved convection in a model with 25 km resolution would be inherently "pathological". We repeated this analysis using a coarse-graining scale of 5 km (10 × 10 WRF points). Results are summarized in Table 1. As expected, the root mean square (RMS) difference between $\bar{p}_{hyd,c}$ and $\bar{p}$ is larger than for the 25 km scale. Nevertheless, even at 5 km the difference between $\bar{p}_{hyd,v}$ and $\bar{p}$ is still much larger than that between $\bar{p}_{hyd,c}$ and $\bar{p}$, suggesting that CL remains more critical at 5 km resolution than nonhydrostatic dynamics.

3.2. Implementation of CL Parameterization in CAM5

[13] In order to quickly assess potential CL impacts, we designed a simple parameterization for CAM5 based on surface precipitation rates. Figure 2 shows a JFD of CL-induced surface pressure, i.e., $p'_{CL} \equiv \bar{p}_{hyd,c} - \bar{p}_{hyd,v}$ at z = 0, and 15-minute average, surface rain rate $\mathcal{R}_{sfc}$ from our WRF simulation. The plot shows that a reasonably-compact, relationship exists between these variables. The additional hydrostatic pressure induced by CL at any height z can be writ ten as

$$p'_{CL}(x,y,z,t) = \int_z^{\infty} g\rho_c^*(x,y,z',t)dz' \quad (5)$$

where ρ_c^* is an effective condensate-induced, perturbation density consistent with p'_{CL} (Figure S1 in the auxiliary material).[1] Examination of ρ_c^* profiles from our WRF simulations binned by $\mathcal{R}_{sfc}$ suggests this density is reasonably constant, or weakly decreasing, from the surface to around 5000 m, and then begins to drop off more sharply

[1] Auxiliary materials are available in the HTML. doi:10.1029/2011GL050533.

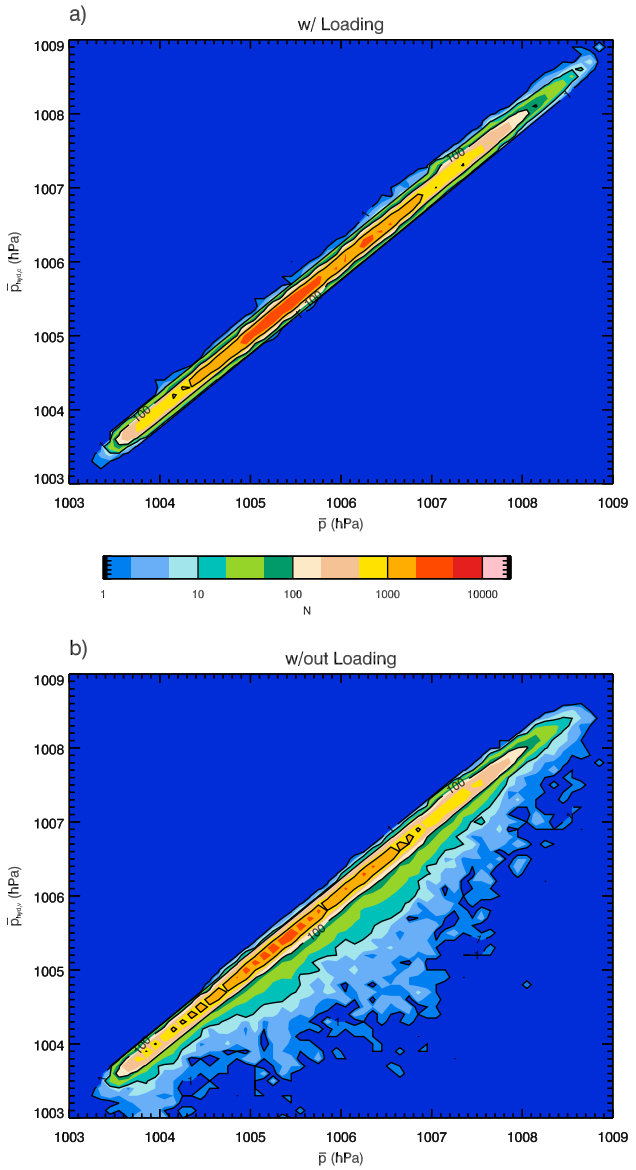

Figure 1. JFDs of WRF pressure $\bar{p}$ (horizontal) vs. diagnostic hydrostatic pressure calculations (vertical). Hydrostatic pressures are calculated using fields coarse-grained to 25 km × 25 km subdomains. (a) Result with a hydrostatic calculation including mass of all condensed species $\bar{p}_{hyd,c}$. (b) Result for hydrostatic calculation ignoring condensate masses $\bar{p}_{hyd,v}$ (see text). N is the number of occurrences in each 0.1 × 0.1 (hPa^2) bin.

between 5000 and 10000 m. This general shape seems to hold for moderate to intense $\mathcal{R}_{sfc}$ (100 to 1000 mm d^{-1}).

[14] As a crude first approximation we set ρ_c^* to a constant value ρ_{c0} between the surface and a height H_{CL} and

Table 1. RMS Differences Between $\bar{p}$ and $\bar{p}_{hyd}$ for Different Coarse-Graining Scales

Coarse-Graining Scale	With Loading (hPa)	Without Loading (hPa)
25 km	0.062	0.17
5 km	0.098	0.25

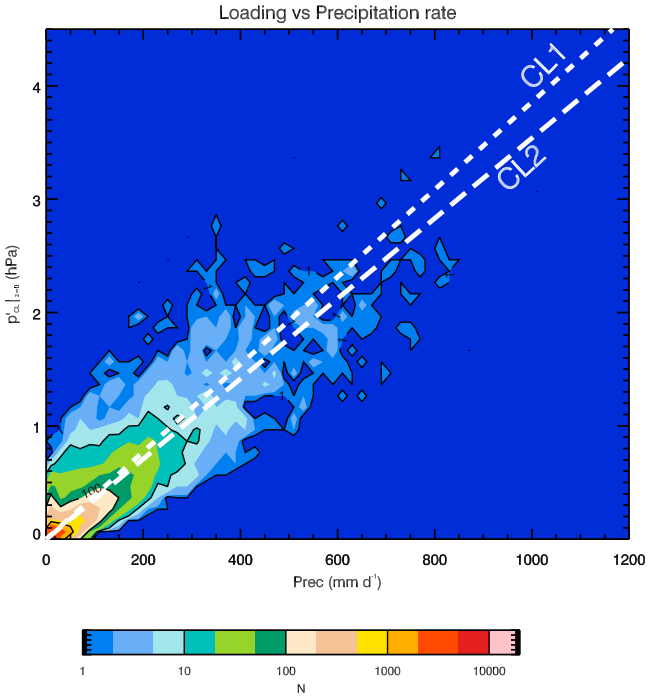

Figure 2. JFD of pressure loading at the surface from condensates (hPa, vertical axis) and surface precipitation rates $\mathcal{R}_{sfc}$ (mm d^{-1}, horizontal axis) in 25 km × 25 km subdomains. Dashed White lines show $p'_{CL}|_{z=0}$ for CL1 and CL2 defined in Table 2. N is the number of occurrences in each 20 × 0.1 (mm d^{-1} × hPa) bin.

set $\rho_c^* = 0$ above. The density ρ_{c0} is then specified as a function of $\mathcal{R}_{sfc}$ and a terminal velocity w_f,

$$\rho_{c0} = \rho_{L0}\frac{\mathcal{R}_{sfc}}{w_f}. \tag{6}$$

where ρ_{L0} is the density of liquid water (1000 kg m^{-3}) and $\mathcal{R}_{sfc}$ is expressed in units of m s^{-1}. Combining (5) and (6) and incorporating our assumptions about the shape of the condensate profile we obtain an expression for the time-varying, fully-3D, hydrostatic pressure perturbation induced by CL

$$p'_{CL}(x,y,z,t) = \begin{cases} g\ \rho_{L0}\dfrac{\mathcal{R}_{sfc}}{w_f} \times (H_{CL} - z) & z \le H_{CL}, \\ 0 & z > H_{CL}. \end{cases} \tag{7}$$

For $\mathcal{R}_{sfc}$ we use the instantaneous CAM5 total surface precipitation (convective + large-scale) at each time step. We simply use the hydrostatically-determined heights of the CAM5 half-levels or layer edges to define the condensate column. When the upper-edge of a layer falls below H_{CL} it is included in the column, otherwise it is left out. This can

Table 2. CAM5 Experiments and Parameters for p'_{CL}

Experiment	w_f	H_{CL}
CTR	control, no loading	control, no loading
CL1	2.5 ms^{-1}	8500 m
CL2	0.625 ms^{-1}	2000 m

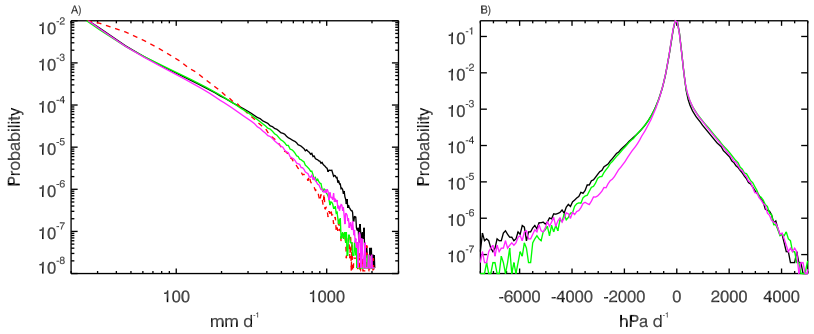

Figure 3. (a) PDFs of precipitation rates for August 2005 between 30°S and 30°N for experiments defined in Table 2: CTR (black curve); CL1 (green curve); and CL2 (magenta curve). The corresponding TRMM 3B42 observational estimate is shown by the dashed red curve. Note results are displayed in log-log form. (b) Same as except for vertical motion around 850 hPa (ω_{850}) over ocean, between 12°S and 25°S. Note only vertical axis is logarithmic in Figure 3b. Probabilities are with respect to bins of 15 mm d^{-1} (Figure 3a) and 80 hPa d^{-1} (Figure 3b).

lead to some variation in the actual thickness of the condensate layers.

[15] The condensate pressure p'_{CL} is added directly to the dynamical pressure in the FV dynamical core immediately before horizontal pressure gradient forces are calculated. In the present implementation p'_{CL} has no other effects in the simulation, so that its horizontal gradient can simply be regarded as another parameterized body force similar to gravity wave drag.

[16] We tried 2 different forms for p'_{CL} (Table 2) whose surface signatures are shown by the white lines in Figure 2. These two experiments are intended to explore the sensitivity of the model to the depth of CL while maintaining the CL pressure signature at the surface approximately constant. Clearly, CL1 with $H_{CL} \approx 8500$ m is closer to the WRF condensate profiles (Figure S1) than is CL2 with $H_{CL} \approx 2000$ m. Note that the specification of H_{CL} is only approximate since actual model layer thicknesses vary in space and time. However, it should be kept in mind that these profiles are from a single 5-day period dominated by deep convection. Furthermore, as will be seen below CL2 reveals interesting sensitivities to H_{CL}.

4. CAM5 Results

[17] Figure 3a shows probability density functions (PDFs) of instantaneous precipitation intensity (30°S–30°N) in our CAM5 experiments, accumulated during August 2005 from data written every 3 hours. The PDF from the CAM5 control (CTR) is shown in black. The observational PDF for precipitation estimated from the Tropical Rainfall Measuring Mission (TRMM) 3B42 product [*Huffman et al.*, 2007] is also shown (dashed red). CTR clearly overestimates the likelihood of precipitation rates greater than 200 mm d^{-1} with respect to TRMM-3B42. There is some uncertainty about whether the TRMM-3B42 precipitation rates represent instantaneous values or longer three hour averages. In any

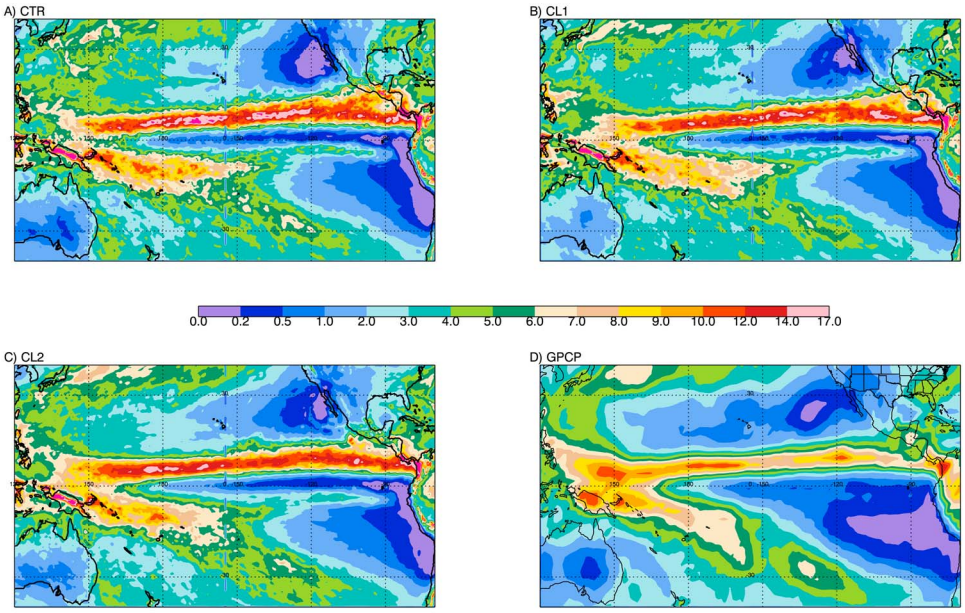

Figure 4. Twelve-month mean surface precipitation rate for 2/2005-1/2006 as a function of longitude and latitude for: (a) CTR; (b) CL1; (c) CL2; and (d) from the GPCP observational estimate.

case, there is minor impact on the model PDFs in Figure 3a when three hour average precipitation rates are used (see Figure S2). *Boyle and Klein* [2010] note that excessive extreme precipitation becomes more pronounced in CAM as resolution increases. We also note that observations of intense precipitation frequency are likely to depend on the area sampled, with smaller sample area yielding more frequent intense events.

[18] With parameterized pressure gradient forces from CL, the frequency of intense precipitation rates ($\mathcal{R}_{sfc}$ > 200 mm d^{-1}) is dramatically reduced. In CL1 only a small excess with respect to TRMM at these rates remains (Figure 3a, green curve). The result for CL2 (magenta curve) is similar to, or even below, that for CL1 for $\mathcal{R}_{sfc}$ < 1000 mm d^{-1}, but at higher rates CL2 is less effective at reducing occurrence probabilities. This suggests that a deep pressure perturbation is better at suppressing these wildly extreme events. In all cases, the effect of CL is remarkably well targeted at reducing the frequency of intense precipitation. At rates below 100 mm d^{-1} little effect from CL is noticeable.

[19] Figure 3b shows PDFs of vertical motion near 850 hPa (ω_{850}) over tropical ocean. There is a clear connection between large precipitation rates and integrated low-level convergence, indicated by $\omega_{850} < 0$. The control simulation exhibits a pronounced skew towards strong convergence events. This skew is significantly reduced in CL1. In CL2 moderate convergence (−4000 to −2000 hPa d^{-1}) is noticeably more suppressed than in CL1, but strong convergence (<−6000 hPa d^{-1}) is almost as frequent as in CTR again suggesting a connection between large H_{CL} and suppression of extremes. A third sensitivity experiment (Figure S3) with H_{CL} comparable to CL1, but with smaller w_f yielded systematically larger reductions in occurrence probability with respect to CL1, at all intensity ranges for both precipitation rates and ω_{850}.

[20] Figure 4 shows 12-month mean precipitation from all CAM5 experiments compared with observational estimates from the Global Precipitation Climatology Project (GPCP) [*Adler et al.*, 2003]. All CAM5 experiments exhibit positive precipitation biases in the Pacific intertropical convergence zone (ITCZ) with respect to GPCP. Modest improvements over CTR (Figure 4a) are evident in CL1 (Figure 4b) particularly south of the Equator where the model's double ITCZ bias has been reduced. Interestingly, in CL2 (Figure 4c) clearer improvements in mean precipitation are seen, with peak values dropping by around 3 mm d^{-1} over much of the northern ITCZ. This suggests that the suppression of moderate low-level convergence seen in Figure 3b may be more significant in determining some aspects of mean model climate than the suppression of extremes.

5. Summary and Discussion

[21] We have shown that a simple but plausible parameterization of condensate loading (CL) has appreciable impacts on simulations with the Community Atmosphere Model version 5 (CAM5) at a horizontal resolution of 0.23°lat × 0.31°lon. Our parameterization assumes a one-to-one relationship between instantaneous surface precipitation rates and the total mass of condensates in the atmospheric column above. The condensates are assumed to have constant density in a layer of specified thickness H_{CL} and to fall with terminal velocity w_f. Three CAM5 experiments with CL were performed using values of w_f and H_{CL} given in Table 2. The surface signatures of the resulting condensate pressure are compared with those from a 5-day cloud resolving simulation of tropical convection using the Weather Research and Forecasting model (WRF) in Figure 2.

[22] The best overall fit to the WRF results (CL1) yields significant reductions in the frequency of intense precipitation ($\mathcal{R}_{sfc}$ > 200 mm d^{-1}) and intense low-level convergence (ω_{850} <−6000 hPa d^{-1}) (Figure 3), as well as modest improvements in annual mean precipitation patterns (Figure 4). Reducing the assumed thickness of the condensate layer (CL2), while maintaining the surface pressure signature close to that in CL1, reduces the impact of CL on the frequency of intense precipitation and convergence. On the other hand, moderate convergence events (Figure 3b) and annual mean precipitation in the ITCZ (Figure 4c) are more strongly suppressed in CL2. This suggests that letting H_{CL} increase with $\mathcal{R}_{sfc}$ could yield improvements in both climate means and extreme event statistics.

[23] We note that our parameter choices in designing the CL parameterization are based on a single 5-day WRF experiment. Both the meteorological background state and the choice of microphysics scheme for the WRF experiment could affect the estimate of CL as a function of surface precipitation rate as well the vertical profile shape chosen to represent the condensates. However, there is no reason to believe that the WRF results used here grossly misrepresent these quantities, and for an exploratory study such as this, we believe this is sufficient.

[24] **Acknowledgments.** NCAR is supported by the National Science Foundation. This work was was also supported by a grant from the Department of Energy's Office of Biological and Environmental Research SciDAC Program. The authors wish to thank the reviewers of our manuscript for their helpful and insightful comments.

[25] The Editor thanks the two anonymous reviewers for their assistance in evaluating this paper.

References

Adler, R., et al. (2003), The Version 2 Global Precipitation Climatology Project (GPCP) monthly precipitation analysis (1979–present), *J. Hydrometeorol.*, *4*(1), 1147–1167.

Boyle, J., and S. A. Klein (2010), Impact of horizontal resolution on climate model forecasts of tropical precipitation and diabatic heating for the TWP-ICE period, *J. Geophys. Res.*, *115*, D23113, doi:10.1029/2010JD014262.

Emanuel, K. (1994), *Atmospheric Convection*, Oxford Univ. Press, New York.

Hong, S., and J. Lim (2006), The WRF single-moment 6-class microphysics scheme (WSM6), *J. Korean Meteorol. Soc*, *42*(2), 129–151.

Huffman, G., et al. (2007), The TRMM Multisatellite Precipitation Analysis (TMPA): Quasi-global, multiyear, combined-sensor precipitation estimates at fine scales, *J. Hydrometeorol.*, *8*(1), 38–55.

Neale, R., et al. (2010), Description of the NCAR Community Atmosphere Model (CAM 5.0), *NCAR Tech. Note NCAR/TN-486+STR*, Natl. Cent. for Atmos. Res., Boulder, Colo.

Skamarock, W., and J. Klemp (2008), A time-split nonhydrostatic atmospheric model for weather research and forecasting applications. *J. Comput. Phys.*, *227*(7), 3465–3485.

Xu, K., and D. Randall (2001), Updraft and downdraft statistics of simulated ropical and midlatitude cumulus convection. *J. Atmos. Sci.*, *58*(13), 1630–1649.

J. T. Bacmeister, A. Dai, P. H. Lauritzen, and J. E. Truesdale, NCAR Earth System Laboratory, National Center for Atmospheric Research, 1850 Table Mesa Dr., Boulder, CO 80305, USA. (juliob@ucar.edu)